MPC-QP-based Control Framework for Compliant Behavior of Humanoid Robots in Physical Collaboration with Humans

Shubham S. Kumbhar and Panagiotis Artemiadis*, *IEEE Senior Member*

***Abstract*— We present a control framework specifically for physical human-humanoid collaboration involving the transportation and manipulation of heavy objects. Using this framework, the humanoid can exhibit desired levels of compliance with the object to be co-transported. This desired compliance is achieved through an admittance model. A Model Predictive Control (MPC) problem, based on a novel Interaction Linear Inverted Pendulum (I-LIP) model, generates footstep patterns that facilitate this desired compliant behavior while keeping the robot stable. Subsequently, we have an object-informed low-level quadratic program (QP) that sends control input to realize the high-level plans on the robot. The stiffness parameters of the I-LIP are modulated in real time for better compliance tracking performance of the robot. We verify all the results through simulation on the humanoid platform, the Digit, showing the prowess of the framework in collaboratively transporting heavy objects with a human.**

I. INTRODUCTION

Humans collaborate with each other daily to achieve common objectives like moving a table from point A to B, or assisting elderly people. This also implies that robots equipped with collaboration capabilities have immense applications and importance. Physical human-robot collaboration (pHRI) involves a human and a robot physically interacting as a unified system to achieve a common goal. These physical interactions can be either direct or indirect through an object. The partnering couple modulates the interaction forces to achieve specific task-based goals. pHRI can also be divided into subtypes like collaboration, competition, and cooperation, as introduced in [1]. According to this taxonomy, this work will belong under the subtype of *cooperation*.

Manipulators have been used extensively for pHRI tasks such as hand-over tasks [2, 3], lifting tasks [4], skill transfer by demonstration [5] and in tasks that involve carrying unknown loads [6]. However, the task space was limited because the robot's base was fixed. A mobile manipulator setup with control strategies to impart compliant motion of the mobile base have been proposed in [7–9]. More recently, works on skill transfer to mobile manipulators for lifting and object carrying tasks [10] and assisted walking [11] have been proposed. However, all these works have a wheeled base that is easily controlled and dynamically more stable than a legged robot.

*This material is based upon work supported by the National Science Foundation under Grants No. 2020009, 2015786, 2025797, and 2018905.

Shubham S. Kumbhar and Panagiotis Artemiadis are with the Mechanical Engineering Department, at the University of Delaware, Newark, DE 19716, USA. shubhamk@udel.edu, partem@udel.edu

*Corrresponding author

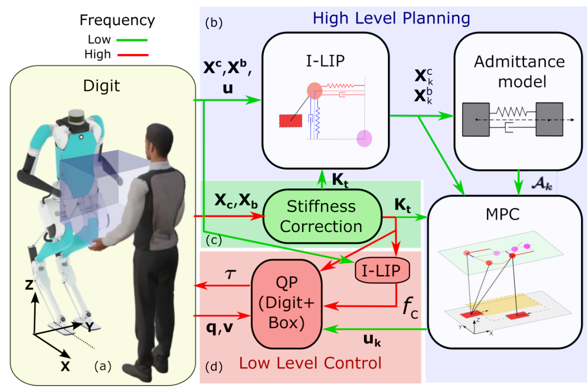

Fig. 1: Complete control framework for physical human-humanoid collaboration showing the Digit robot collaborating with a human to transfer a box. The three components of the proposed framework are shown: high-level planning, stiffness modulation, and low-level control

The versatility and maneuverability of legged locomotion in human-human collaboration motivate pHRI robots to have legged bases. A humanoid robot with motion, sensing, and actuation capabilities similar to those of a human partner has excellent potential for effective collaboration with humans, especially in environments designed for human use. However, this versatility comes with the challenge of ensuring control and stability for these types of robots.

One of the first works in pHRI using a humanoid robot, the HRP-2P, was done by authors in [12] to move a panel collaboratively. The authors in [13] developed a framework for humanoids that combine visions and haptic information for collaborative tasks. Current humanoid walking research is divided into two levels: high-level planning for global center of mass (COM) trajectories and foot placements, and low-level or joint-level execution. Model Predictive Control (MPC) is commonly used for high-level planning, utilizing models like the Linear Inverted Pendulum (LIP) [14, 15] and Single Rigid Body (SRB) [16]. Low-level control typically employs quadratic programs (QP) [14, 17].

The work in [18] employs a high-level MPC with admittance control of the COM added in the cost function to generate footstep patterns. However, the wrench used is transformed to the COM frame, assuming quasi-static motion, and is also predicted to remain constant over the horizon of the MPC. The admittance model sets a desired impedance between the robot's COM and the origin, requiring significant effort from the human to move the robot and thus making it unsuitable for mobile tasks. In [19], these high-level plans are tracked using a quadratic program that also takes external forces into account. Knowledge of these external forces in the QP helps generate compensatory actions required to track trajectories and stay stable. However, these forces are not controlled or planned by the robot, giving it no ability to actively control the object carried with the human, a box, or keep the interaction forces low. The robot is also unaware of the object's state. Neither of these works present results on the compliant behavior of the robot about the box.

To the best of our knowledge, this paper is the first work that presents a comprehensive pHRI control framework for achieving different levels of compliance between a humanoid robot and the object for tasks that involve collaborative object transportation, as shown in Fig. 1. We have an admittance model that dictates the desired compliant behavior. We formulate a walking pattern generator as an MPC that uses a novel simplified model, the Interaction Linear Inverted Pendulum (I-LIP). Additionally, our framework incorporates a low-level quadratic program that considers the dynamics of the object, enabling effective control of the interaction forces and the object's position and orientation. By adjusting the interaction forces, we can control how much the legged base actively contributes to achieving the desired compliant behavior. For instance, when the interaction forces are constrained to be low, the footstep pattern can become the primary effort towards the compliant behavior. To ensure accurate, compliant behavior tracking, we propose a gain correction strategy for adjusting the spring constant and damping parameters of the I-LIP. Another crucial point to highlight is that the load transported in this work is a box weighing 20 Kg. Notably, existing literature lacks studies addressing objects of this considerable weight, which typically require the physical effort of two individuals to maneuver.

II. High Level Planning

We consider tasks in which the Digit collaboratively transfers an object (box) with a human. Without loss of generality, the framework in this paper will focus on the human, and therefore, the box, moving in a straight line. The forward and the lateral direction of motion are the X and Y axes shown in Fig. 2(a). Let $\mathbf{x}^{\mathrm{c}} = [x^{\mathrm{c}}, y^{\mathrm{c}}]^{\mathrm{T}}$ and $\dot{\mathbf{x}}^{\mathrm{c}} = [\dot{x}^{\mathrm{c}}, \dot{y}^{\mathrm{c}}]^{\mathrm{T}}$ be the Digit's COM X and Y component position and velocity respectively. Let $\mathbf{u} = [u^{\mathrm{x}}, u^{\mathrm{y}}]^{\mathrm{T}}$ be the position of the stance foot. We assume that the Z-component of all foot strikes is zero. Let $\mathbf{x}^{\mathrm{b}} = [x^{\mathrm{b}}, y^{\mathrm{b}}]^{\mathrm{T}}$ and $\dot{\mathbf{x}}^{\mathrm{b}} = [\dot{x}^{\mathrm{b}}, \dot{y}^{\mathrm{b}}]^{\mathrm{T}}$ be the object's X and Y component position and velocity respectively. Let $\mathbf{X}^{\mathrm{c}} = [\mathbf{x}^{\mathrm{c}}, \dot{\mathbf{x}}^{\mathrm{c}}]^{\mathrm{T}}$ and $\mathbf{X}^{\mathrm{b}} = [\mathbf{x}^{\mathrm{b}}, \dot{\mathbf{x}}^{\mathrm{b}}]^{\mathrm{T}}$ be the concatenated state vectors of positions and velocities. As shown in Fig. 1, the high level planning block takes the set $\{\mathbf{X}^{\mathrm{c}}, \mathbf{X}^{\mathrm{b}}, \mathbf{u}\}$ as input for further computations in the I-LIP, the admittance model and the MPC blocks, as explained below. It is also assumed that the human wants to move the object with a constant desired velocity. This velocity is unknown to the robot and is estimated by the controller in real time using exponential moving average [20]. We denote this estimated desired velocity using $\mathbf{v}^{\mathrm{b}}_{\mathrm{d}} = [v^{\mathrm{bx}}_{\mathrm{d}}, v^{\mathrm{by}}_{\mathrm{d}}]^{\mathrm{T}}$. Since, we already know that the task is limited to straight line walking, we set $v^{\mathrm{by}}_{\mathrm{d}} = 0$.

A. Interaction Linear Inverted Pendulum (I-LIP)

Figure 2(a) depicts the Interaction Linear Inverted Pendulum (I-LIP) model used for predicting the evolution of the robot's COM. It is an extension to the Linear Inverted Pendulum (LIP) model [15] to make the footstep and COM planning aware of the interaction forces and motion of the object. The I-LIP consists of a massless prismatic leg and two point masses representing the COM of the robot and the object. One end of the leg is pivoting about the contact point on the ground, and the other is connected to the point mass representing the COM of robot. Furthermore, the two point masses are connected using springs and dampers in the X and Y directions, as shown in Fig. 2(b). The k^{th} step of the I-LIP occurs in the time interval $[kT, (k+1)T)$ between two consecutive foot strikes. Here, T is the duration of a step. In Fig. 2(a,b), $\mathbf{u}_{\mathrm{k}} = \mathbf{u}(t = kT)$ represents the position of the stance foot ($\mathbf{u}$) during the k^{th} step. $\mathbf{X}^{\mathrm{c}}_{\mathrm{k}} = \mathbf{X}^{\mathrm{c}}(t = kT)$ and $\mathbf{X}^{\mathrm{b}}_{\mathrm{k}} = \mathbf{X}^{\mathrm{b}}(t = kT)$ represent the COM state vectors of robot ($\mathbf{X}^{\mathrm{c}}$) and object ($\mathbf{X}^{\mathrm{b}}$) respectively at the start of the k^{th} step. Similarly, $\mathbf{X}^{\mathrm{c}}_{\mathrm{k+1}}$ and $\mathbf{X}^{\mathrm{b}}_{\mathrm{k+1}}$ represent the COM state vectors of robot and object respectively at the start of the $(k+1)^{\mathrm{th}}$ step. $\mathbf{u}_{\mathrm{k+1}}$ represents the stance foot position during the $(k+1)^{\mathrm{th}}$ step. The stepping pattern alternates between the left and the right foot and so if $\mathbf{u}_{\mathrm{k}}$ is the left stance foot, then, $\mathbf{u}_{\mathrm{k+1}}$ is the right stance foot.

The I-LIP assumes that the human is moving the object with a constant intended velocity. This unknown velocity is estimated and denoted by $\mathbf{v}^{\mathrm{b}}_{\mathrm{d}}$ as discussed above. Under this assumption, the dynamics of the COM of the robot in I-LIP are described by

$$\begin{aligned}\mathrm{m_c}\ddot{\mathbf{x}}^{\mathrm{c}} = \mathrm{m_c}\omega_{\mathrm{o}}^2(\mathbf{x}^{c} - \mathbf{u}) + \mathbf{B}(\mathbf{v}^{\mathrm{b}}_{\mathrm{d}} - \dot{\mathbf{x}}^{\mathrm{c}})\\ + \mathbf{K}_{\mathrm{t}}(\mathbf{x}^{\mathrm{b}}_{\mathrm{init}} + \mathbf{v}^{\mathrm{b}}t - \mathbf{x}^{c} - \mathbf{x}^{\mathrm{d}}_{\mathrm{m}})\end{aligned} \quad (1)$$

where $\omega_{\mathrm{o}} = \sqrt{g/h}$, g is the magnitude of the gravitational acceleration, $\mathbf{x}^{\mathrm{b}}_{\mathrm{init}}$ is the initial position of the COM of the object, and $\mathbf{x}^{\mathrm{d}}_{\mathrm{m}}$ is the x-y component natural length of the spring. $\mathbf{K}_t = diag(K^{\mathrm{x}}_t, K^{\mathrm{y}})$ is the spring constant matrix at the instant the high-level planner is initiated, and $\mathbf{B} = diag(B^{\mathrm{x}}, B^{\mathrm{y}})$ is the damping constant matrix. The stiffness of the x-component spring is modulated in real time in the stiffness modulation block in Fig. 1. The subscript t in $\mathbf{K}_t$ indicates the stiffness of the springs at the instant when the high level planner is invoked and remains constant until the high level planning is complete. Using the analytical solutions of the non-homogeneous linear differential equations (1), we can get the step-to-step discrete dynamics of I-LIP.

$$\mathbf{X}^{\mathrm{c}}_{k+1} = f_{\mathrm{c}}(\mathbf{X}^{\mathrm{c}}_{k}, \mathbf{x}^{\mathrm{b}}_{k}, \mathbf{v}^{\mathrm{b}}_{\mathrm{d}}, \mathbf{u}_{k}, \mathbf{K}_t, T) \quad (2)$$

The step-to-step evolution of the COM of the object is given by:

$$\mathbf{X}^{\mathrm{b}}_{k+1} = f_{\mathrm{b}}(\mathbf{x}^{\mathrm{b}}_{k}, \mathbf{v}^{\mathrm{b}}_{\mathrm{d}}, T) = \begin{bmatrix}\mathbf{x}^{\mathrm{b}}_{k} + \mathbf{v}^{\mathrm{b}}_{\mathrm{d}}T\\ \mathbf{v}^{\mathrm{b}}_{\mathrm{d}}\end{bmatrix} \quad (3)$$

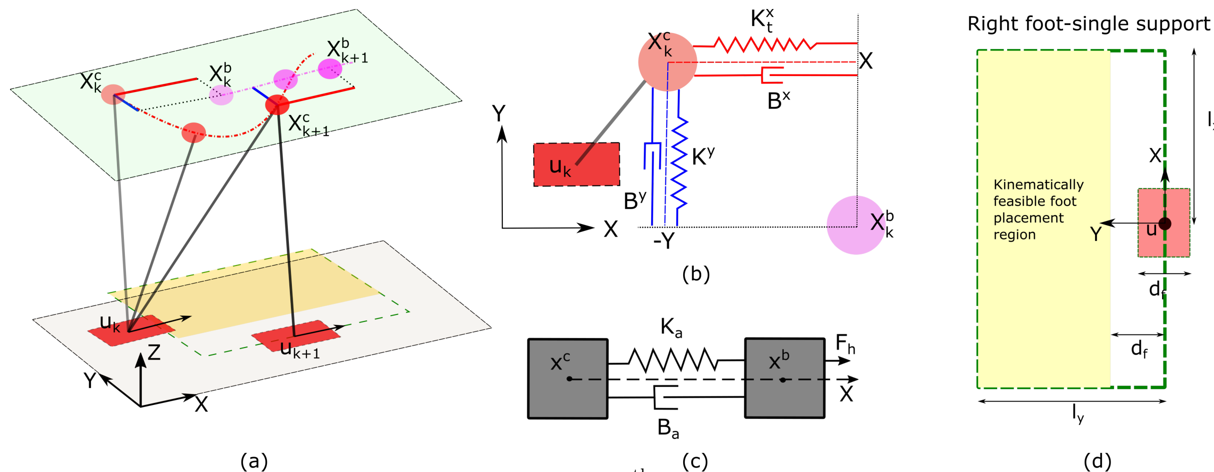

Fig. 2: (a) Interaction Linear Inverted Pendulum (I-LIP) during the k^{th} step with left leg as the stance foot ($\mathbf{u}_k$). Here the red and blue solid lines represent the springs and dampers in the X and Y directions. The dashed red line represents the evolution trajectory of the robot's COM. Similarly, the purple dashed line represents the evolution trajectory of the object's COM. Decreasing transparency indicates forward propagation in time. The red rectangle is the stance foot and the yellow rectangle represents the admissible region for the next foot placement. (b) Top view of the I-LIP at the start of the k^{th} step showing the springs and dampers; (c) The admittance model, which consists of two point masses connected through a spring and damper; (d) The yellow region denotes the kinematically feasible region for the next foot placement, given the I-LIP is currently on the right stance foot.

Given that we are in the $(k-1)^{\text{th}}$ step, the I-LIP block in Fig. 1(b) consists of predicting the COM state of the robot and the object at the end of the step using the function f_{a} and f_{b} as $\mathbf{X}^{\text{c}}_k = f_{\text{c}}(\mathbf{X}^{\text{c}}, \mathbf{x}^{\text{b}}, \mathbf{v}^{\text{b}}_{\text{d}}, \mathbf{u}, \mathbf{K}_t, (1-s)T)$ and $\mathbf{X}^{\text{b}}_k = f_{\text{b}}(\mathbf{x}^{\text{b}}, \mathbf{v}^{\text{b}}_{\text{d}}, (1-s)T)$. Here, $s = (t-(k-1)T)/T$ is a variable given by the ratio of time passed since the start of the step to total step time, T. As shown in Fig.1(b) the predicted set, $\{\mathbf{X}^{\text{c}}_{\text{k}}, \mathbf{X}^{\text{b}}_{\text{k}}\}$ is used by the admittance model and the MPC blocks for further planning.

Before moving on to the admittance model, we briefly discuss certain functional details of the I-LIP. Due to limited capabilities of the robot, we put constraints on where the next foot can be placed. Fig. 2(d) shows the feasible foot placement region for the next step of the I-LIP. The feasible foot placement region is parameterized using the following parameters: a) l_x: Maximum footstep length in the forward direction, b) l_y: Maximum footstep in the lateral direction, c) d_f: Foot width. The region is given by the following set:

$$\begin{aligned}\boldsymbol{\mathcal{U}}_k =&\{(u^x_k, u^y_k) \mid -l_x \le (u^x_k - u^x_{k-1}) \le l_x \\ &\text{and } d_f \le m(u^x_k - u^x_{k-1}) \le l_y\}\end{aligned} \tag{4}$$

Here, $m = 1$ if the stance foot is the right foot, and -1 otherwise. For the lateral or Y-direction, we have an additional constraint that the left and the right legs cannot cross each other. We also provide a clearance equal to the foot width to avoid collision of the swing foot with the stance foot.

B. Admittance Model

The admittance model is a one-dimensional model comprising of two masses connected through a spring and a damper, as shown in Fig. 2(c). The robot and the object are modeled as point masses with mass $\mathrm{m_c}$ and $\mathrm{m_b}$ respectively. Let x^{c} and $\dot{x}^{\text{c}}$ be the x-component position and velocity of the COM of the robot. Similarly, let x^{b} and $\dot{x}^{\text{b}}$ be the x-component position and velocity of the COM of the object. The spring and the damper are for a compliant response of the robot with respect to the object. We also assume that the object is moving with a constant velocity of v^{bx}_{d}. Under this assumption, the dynamics of the COM of the robot in the admittance model are given by:

$$m_{\text{c}}\ddot{x}^c = K_{\text{a}}(x^{\text{b}} - x^{\text{c}} - x^{\text{d}}) + B_{\text{a}}(v^{\text{bx}}_{\text{d}} - \dot{x}^{\text{c}}) \tag{5}$$

Here, $x^{\text{b}} = x^{\text{b}}_{\text{init}} + v^{\text{bx}}_{\text{d}} t$ with $\mathbf{x}^{\text{b}}_{\text{init}}$ being the initial position of the COM of the object. Let $x^{\text{c}}_k = x^{\text{c}}(t = kT)$ and $\dot{x}^{\text{c}}_k = \dot{x}^{\text{c}}(t = kT)$ be the position and velocity of the COM of the robot at the start of the k^{th} step. Similarly, let $x^{\text{b}}_k = x^{\text{b}}(t = kT)$ be the position of the COM of the object at the start of the k^{th} step. Using the analytical solution of the non-homogeneous differential equation (5), we can get a function f_{a} that maps the state of the robot's COM at the start of the k^{th} step $(x^{\text{c}}_k, \dot{x}^{\text{c}}_k)$ to the state at the start of the $(k+1)^{\text{th}}$ step $(x^{\text{c}}_{k+1}, \dot{x}^{\text{c}}_{k+1})$:

$$x^{\text{c}}_{\text{k+1}}, \dot{x}^{\text{c}}_{\text{k+1}} = f_{\text{a}}(x^{\text{c}}_{\text{k}}, \dot{x}^{\text{c}}_{\text{k}}, x^{\text{b}}_{\text{k}}, v^{\text{bx}}_{\text{d}}, T) \tag{6}$$

Using $\mathbf{X}^{\text{c}}_{\text{k}}$ and $\mathbf{X}^{\text{b}}_{\text{k}}$ as input as shown in Fig. 1(b), specifically the x-components, and (6), the admittance model block computes, $x^{\text{c}}_{\text{a}}(k+i) = x^{\text{c}}_{\text{k+i}}$ and $\dot{x}^{\text{c}}_{\text{a}}(k+i) = \dot{x}^{\text{c}}_{\text{k+i}}\ \forall\ i = 1, 2, ..\text{N}$. Here, N is the horizon of the MPC and means the number of future steps of prediction. Let the output of this block be denoted by the set $\boldsymbol{\mathcal{A}_k}$, where:

$$\boldsymbol{\mathcal{A}_k} = \bigcup_{i=1}^{\text{N}} \{x^{\text{c}}_{\text{a}}(k+i)\} \tag{7}$$

This set is passed on as goal positions in the MPC formulation that uses I-LIP.

C. Model Predictive control

In this subsection, we formulate the walking pattern generator as a model predictive control (MPC) problem. MPC is formulated as a quadratic optimization with constraints on foot placement and COM states. Given the initial COM states of the object and the robot, the goal is to find N future optimal foot placements of the I-LIP model that lead to optimal tracking of the desired robot's COM positions. The MPC, as shown in Fig. 1(b) uses $(\mathbf{X}^{\mathrm{c}}_{\mathrm{k}}, \mathbf{X}^{\mathrm{b}}_{\mathrm{k}})$, the goal states $(\boldsymbol{\mathcal{A}_k})$ and $\mathbf{K}_t$ to output the stance foot x-y position of the next footstep $(\mathbf{u}_k)$. The formulation is as follows:

$$\underset{\mathbf{X}^{\mathrm{c}}_{i+1}, \mathbf{u}_i}{\text{minimize}} \quad \sum_{i=k}^{k+N-1} J_i(\mathbf{x}^{\mathrm{c}}_i, \mathbf{u}_{i-1}) \tag{8}$$

$$\text{subject to} \quad \mathbf{X}^{\mathrm{c}}_{k+1} = f_{\mathrm{c}}(\mathbf{X}^{\mathrm{c}}_k, \mathbf{x}^{\mathrm{b}}_k, \mathbf{v}^{\mathrm{b}}_{\mathrm{d}}, \mathbf{u}_k, \mathbf{K}_t, T) \tag{9}$$

$$\mathbf{u}_i = (u^x_i, u^y_i) \in \mathcal{U}_i \tag{10}$$

The decision variables of this optimization are the robot's COM states, $\mathbf{X}^{c}_{i+1}$ and $\mathbf{u}_i \ \forall \ i \in \{k, k+1, \ldots, k+N-1\}$. The two constraints are the step-to-step dynamics of I-LIP (9), and the foot placement constraint (10). The cost, J_i is formulated as a weighted sum of two individual costs $\Phi_{k,1}$ and $\Phi_{k,2}$ defined below.

1) Goal position tracking: This objective is used to generate footstep patterns that reduce the error between the robot's COM position and the goal positions. Let the goal position at the start of the k^{th} step be denoted by $\mathbf{x}^{\mathrm{c}}_g(k)$ and be given by $(x^{\mathrm{c}}_{\mathrm{a}}(k), 0)$. $x^{\mathrm{c}}_{\mathrm{a}}(k)$ comes from (7) and the desired y position is set to zero. The cost is defined as:

$$\Phi_{k,1} = (\mathbf{x}^{\mathrm{c}}_k - \mathbf{x}^{\mathrm{c}}_{\mathrm{g}}(k))^T \mathbf{K}_{\Phi} (\mathbf{x}^{\mathrm{c}}_k - \mathbf{x}^{\mathrm{c}}_{\mathrm{g}}(k)) \tag{11}$$

where $\mathbf{K}_{\Phi}$ is a positive definite diagonal gain matrix.

2) COM-foot distance regulation: The second cost is to minimize the distance between the COM of the robot and the stance foot at the end of the step. This is done so that the footsteps taken do not lead to increased distance between COM and the foot, which can cause the robot to fall. This can also be seen in the work done on the capture point for the Linear Inverted Pendulum (LIP) [21]. The farther the capture point from the foot, the closer it is to a fall. The cost for our case is defined as:

$$\Phi_{k,2} = (\mathbf{x}^{\mathrm{c}}_k - \mathbf{u}_{k-1})^T \mathbf{B}_{\Phi} (\mathbf{x}^{\mathrm{c}}_k - \mathbf{u}_{k-1}) \tag{12}$$

where $\mathbf{B}_{\Phi}$ is a positive definite diagonal gain matrix. The term J_i is given as, $J_i(\mathbf{x}^{\mathrm{c}}_i, \mathbf{u}_{i-1}) = \phi_1 \Phi_{k,1} + \phi_2 \Phi_{k,2}$, where ϕ_1 and ϕ_2 are weights selected based on the priority of each cost. Once the MPC is solved, the next planned footstep location $(\mathbf{u}_k)$ is sent to the low level control for foot placement tracking as shown in Fig. 1.

III. Low Level Control

The goal of the low-level control is to realize the high-level plan given by MPC on the Digit. As shown in Fig. 1(d), it has two steps: (a) I-LIP block: We get the desired COM state of the robot at the current instant by integrating the I-LIP dynamics from the previous instant of low level control. Let the time between two consecutive instances of low level control be δt. Let $\mathbf{X}^{\mathrm{c}}_{\mathrm{d}} = [\mathbf{x}^{\mathrm{c}}_{\mathrm{d}}, \dot{\mathbf{x}}^{\mathrm{c}}_{\mathrm{d}}]^{\mathrm{T}}$ be the desired state vector of robot's COM. Here, $\mathbf{x}^{\mathrm{c}}_{\mathrm{d}}$ and $\dot{\mathbf{x}}^{\mathrm{c}}_{\mathrm{d}}$ are the desired X and Y components of position and velocity of the robot's COM respectively. Similarly, let $\mathbf{X}^{\mathrm{b}}_{\mathrm{d}} = [\mathbf{x}^{\mathrm{b}}_{\mathrm{d}}, \dot{\mathbf{x}}^{\mathrm{b}}_{\mathrm{d}}]^{\mathrm{T}}$ be the desired state vector of the object's COM. We use the function f_{c} from (2) and f_{b} from (3) to get the desired COM state of the robot and the object as:

$$\mathbf{X}^{\mathrm{c}}_{\mathrm{d}}(t) = f_{\mathrm{c}}(\mathbf{X}^{\mathrm{c}}_{\mathrm{d}}(t-\delta t), \mathbf{x}^{\mathrm{b}}_{\mathrm{d}}(t-\delta t), \mathbf{v}^{\mathrm{b}}_{\mathrm{d}}, \mathbf{u}, \mathbf{K}_t, \delta t) \tag{13}$$

$$\mathbf{X}^{\mathrm{b}}_{\mathrm{d}}(t) = f_{\mathrm{b}}(\mathbf{x}^{\mathrm{b}}_{\mathrm{d}}(t-\delta t), \mathbf{v}^{\mathrm{b}}_{\mathrm{d}}, \delta t) \tag{14}$$

The desired states, $\mathbf{X}^{\mathrm{c}}_{\mathrm{d}}$ and $\mathbf{X}^{\mathrm{b}}_{\mathrm{d}}$ are reset to the current state of the system, i.e., $\mathbf{X}^{\mathrm{c}}_{\mathrm{d}}(t) = \mathbf{X}^{\mathrm{c}}(t)$ and $\mathbf{X}^{\mathrm{b}}_{\mathrm{d}}(t) = \mathbf{X}^{\mathrm{b}}(t)$ at every instant the high level planner is invoked. b) QP block: Let be $\mathbf{q}$ and $\mathbf{v}$ be the generalized joint coordinates and velocities of the coupled system consisting of the Digit and the object. As shown in Fig. 1(d), the quadratic program (QP) takes the above explained desired COM plan $(\mathbf{X}^{\mathrm{c}}_{\mathrm{d}}(t))$, the current state of the system $(\mathbf{q}, \mathbf{v})$, forces applied by the human, and footstep plan $(\mathbf{u}_k)$ from MPC to output joint torque commands $(\boldsymbol{\tau})$ to be sent to Digit. We describe the constraints and objectives of the QP below.

A. Constraints

The dynamics of the coupled system are incorporated as constraints in the optimization so that the solutions given by the low-level control can be realized on Digit. The literature on whole-body control for pHRI typically considers interaction forces as external forces within the system's dynamics, but does not actively plan for these forces. In contrast, our approach incorporates the dynamics of the coupled system—comprising both the robot (Digit) and the object, allowing the robot to actively control interaction forces. This method also provides the flexibility to manage both the orientation and position of the object.

In our walking dynamics, we alternate between left and right single support phases and assume that the double support phase is of negligible time. The dynamics of the Digit during the single support phase are given by:

$$\begin{aligned} \mathbf{D}(\mathbf{q})\dot{\mathbf{v}} + \mathbf{C}(\mathbf{q}, \mathbf{v}) =& \mathbf{S}^{\mathrm{T}}_{\tau} \boldsymbol{\tau} + \mathbf{J}^{\mathrm{T}}(\mathbf{q}) \boldsymbol{\lambda} \\ &+ \mathbf{J}^{\mathrm{T}}_{\mathrm{L}}(\mathbf{q}) \boldsymbol{\lambda}_{\mathrm{L}} + \mathbf{J}^{\mathrm{T}}_{\mathrm{R}}(\mathbf{q}) \boldsymbol{\lambda}_{\mathrm{R}} \end{aligned} \tag{15}$$

Here, $\mathbf{D}(\mathbf{q})$ is the inertia matrix, $\mathbf{C}(\mathbf{q}, \mathbf{v})$ is the matrix containing velocity-dependent terms and gravitational forces and $\mathbf{S}_{\tau}$ is the matrix that selects the joints that are actuated. $\mathbf{J}_L(\mathbf{q})$ is the jacobian of ball joint constraint between the left hand and the object and $\boldsymbol{\lambda}_{\mathrm{L}} = [\lambda^{\mathrm{x}}_{\mathrm{L}}, \lambda^{\mathrm{y}}_{\mathrm{L}}, \lambda^{\mathrm{z}}_{\mathrm{L}}]^{\mathrm{T}} \in \mathbb{R}^3$ is the corresponding generalized force. We use a similar notation for the right hand but with the 'R' subscript. $\mathbf{J}(q)$ is the jacobian of all the holonomic constraints apart from the ones with the box, and $\lambda \in \mathbb{R}^{16}$ are the corresponding constraint generalized forces. These constraints include a) six closed-loop constraints due to the Digit's structure, b) Stance foot contact constraint, and c) Stiff spring constraints. The closed loop kinematic constraints are handled similarly to Cassie robot [22]. All these constraints are incorporated as:

$$\mathbf{J}(q)\dot{\mathbf{v}} + \dot{\mathbf{J}}(\mathbf{q}, \mathbf{v})\mathbf{v} = \mathbf{0} \tag{16}$$

Next, we include the dynamics of the object, which is modeled as a single rigid body. Let $\boldsymbol{\alpha}_{\mathrm{b}}$ and $\boldsymbol{\omega}_{\mathrm{b}}$ be the angular acceleration and velocity of the object in the world frame. We use $\mathbf{I}_{\mathrm{b}}$ and m_{b} to denote the moment of inertia matrix in the body frame and mass of the object, respectively. Let $\mathbf{F}_{\mathrm{h}}$ and $\mathbf{M}_{\mathrm{h}}$ be the net forces and moments applied by the human at the center of the object in the world frame. Let $\mathbf{R} \in SO(3)$ be the rotation matrix to transform from the object frame to the world frame and $\mathbf{F}_{\mathrm{g}}$ be the force due to gravity. Let $\mathbf{r}_{\mathrm{L}}$ and $\mathbf{r}_{\mathrm{R}}$ denote vectors in the world frame for the position of left-hand and right-hand point of contact with the object relative to the COM frame of the object. The dynamics of the object are given by:

$$\mathbf{M}_{\mathrm{h}} - \mathbf{r}_{\mathrm{L}} \times \boldsymbol{\lambda}_{\mathrm{L}} - \mathbf{r}_{\mathrm{R}} \times \boldsymbol{\lambda}_{\mathrm{R}} = \mathbf{R}\mathbf{I}_{\mathrm{b}}\mathbf{R}^T\boldsymbol{\alpha}_{\mathrm{b}} + \boldsymbol{\omega}_{\mathrm{b}} \times \mathbf{R}\mathbf{I}_{\mathrm{b}}\mathbf{R}^T\boldsymbol{\omega}_{\mathrm{b}} \quad (17)$$

$$m_{\mathrm{b}}\ddot{\mathbf{x}}^{\mathrm{b}} = \mathbf{F}_{\mathrm{g}} - \boldsymbol{\lambda}_{\mathrm{L}} - \boldsymbol{\lambda}_{\mathrm{R}} + \mathbf{F}_{\mathrm{h}} \quad (18)$$

Finally, we add 2 ball joint constraints between the two arms and the object:

$$\mathbf{J}_i(\mathbf{q})\dot{\mathbf{v}} + \dot{\mathbf{J}}_i(\mathbf{q},\mathbf{v})\mathbf{v} = \ddot{\mathbf{x}}^{\mathrm{b}} + \mathbf{r}_i \times \boldsymbol{\alpha}_{\mathrm{b}} + \boldsymbol{\omega}_{\mathrm{b}} \times (\boldsymbol{\omega}_{\mathrm{b}} \times \mathbf{r}_i) \ \forall\ i \in \{\mathrm{L},\mathrm{R}\} \quad (19)$$

Next, we require the foot contact wrench, $(\lambda^x, \lambda^y, \lambda^z, \lambda^{mx}, \lambda^{my}, \lambda^{mz})$ to lie inside the linearized Contact Wrench Cone (CWC) $\mathcal{K}$ [23]. We also bound the input torque and interaction forces at the hands as:

$$\mathbf{lb}_\tau \leq \boldsymbol{\tau} \leq \mathbf{ub}_\tau \quad (20)$$

$$\mathbf{lb}_{\mathrm{h}} \leq \boldsymbol{\lambda}_i \leq \mathbf{ub}_{\mathrm{h}} \ \forall\ i \in \{L, R\} \quad (21)$$

Here, $\mathbf{lb}_\tau$ and $\mathbf{ub}_\tau$ are the lower and upper bounds on the input torque, $\boldsymbol{\tau}$. Moreover, $\mathbf{lb}_{\mathrm{h}}$ and $\mathbf{ub}_{\mathrm{h}}$ are the lower and upper bounds on the interaction forces between the box and the hand.

B. Objectives

1) Trajectory Tracking Objectives: Here, we discuss the objectives that pertain to tracking desired trajectories of different variables. These include tracking the desired Digit's COM position, swing foot position, swing foot orientation, object height, and torso orientation. Let the errors between the desired and actual values of these variables be stacked into a vector, $\mathbf{e} \in \mathbb{R}^{13}$. The objective then is to minimize Ψ_1, defined as: $\Psi_1 = ||\ddot{\mathbf{e}} + \mathbf{K}_{\mathrm{D}}\dot{\mathbf{e}} + \mathbf{K}_{\mathrm{P}}\mathbf{e}||^2$. Here, $\mathbf{K}_{\mathrm{D}}$ and $\mathbf{K}_{\mathrm{P}}$ are appropriately selected gain matrices. The desired Digit's COM state is given by $\mathbf{X}^{\mathrm{c}}_{\mathrm{d}}(t)$ as discussed above. The desired COM acceleration is found by substituting $\mathbf{X}^{\mathrm{c}}_{\mathrm{d}}(t)$ in (1). The swing foot trajectory and orientation errors are the same as defined in [14]. An identity quaternion orientation is desired for the torso. It must be noted that we do not aim to control the robot in manipulating the x and y position and orientation of the box, as we want to avoid excessive interaction forces that may arise from a mismatch between human and robot intentions.

2) Other Objectives: The COM in I-LIP is a point mass and cannot capture the effects of angular momentum on Digit. We, therefore, minimize the angular momentum as done in [14]. Specifically, we compute the angular momentum of the digit about its COM, $\boldsymbol{\eta}_2 = \mathbf{A}_{\mathrm{ang}}\mathbf{v}$. Let $\mathbf{A}_{\mathrm{ang}}$ be the angular part of the centroidal momentum matrix. The minimization objective is given by: $\Psi_2 = ||\dot{\boldsymbol{\eta}}_2 + \mathbf{K}_{\mathrm{ang}}\boldsymbol{\eta}_2||^2$, where $\mathbf{K}_{\mathrm{ang}}$ is appropriately selected gain matrix. Next, we also minimize the input torque as: $\Psi_3 = ||\boldsymbol{\tau}||^2$. We also minimize the x and y direction forces at the point of interaction between the box and the arms of the robot by using: $\Psi_4 = \beta||\lambda^{\mathrm{x}}_{\mathrm{L}}||^2 + \beta||\lambda^{\mathrm{x}}_{\mathrm{R}}||^2 + ||\lambda^{\mathrm{y}}_{\mathrm{L}}||^2 + ||\lambda^{\mathrm{y}}_{\mathrm{R}}||^2$, where β is an appropriately selected weight for the x-component forces. This helps to keep the interaction forces minimal so that the human does not have to apply excessive amounts of force in the x and y directions to overcome the resistance of the robot. We also try to equalize the z-direction interaction forces on the left and right hand so that the roll of the box is minimized: $\Psi_5 = ||\lambda^{\mathrm{z}}_{\mathrm{L}} - \lambda^{\mathrm{z}}_{\mathrm{R}}||^2$.

C. Weighted QP

To formulate the optimization problem, we take a weighted sum of the above-described objectives and combine it into a single quadratic objective. Using this objective and the constraints, the QP is formulated as:

$$\underset{\dot{\mathbf{v}},\ddot{\mathbf{x}}_b,\boldsymbol{\alpha}_{\mathrm{b}},\boldsymbol{\tau},\boldsymbol{\lambda},\boldsymbol{\lambda}^{\mathrm{L}},\boldsymbol{\lambda}^{\mathrm{R}}}{\text{minimize}} \quad \psi_1\Psi_1 + \psi_2\Psi_2 + \psi_3\Psi_3 + \psi_4\Psi_4 + \psi_5\Psi_5 \quad (22)$$

$$\text{subject to} \quad (15), (16), (17), (18), (19), (20), (21)$$
$$(\lambda^x, \lambda^y, \lambda^z, \lambda^{mx}, \lambda^{my}, \lambda^{mz}) \in \mathcal{K} \quad (23)$$

The gains, $\psi_i\ \forall i \in \{1, 2, 3, 4, 5\}$ are selected depending on the priority of the objectives. The last constraint is on the contact wrench of the stance foot. It is required to lie inside the Linearized Contact Wrench Cone, $\mathcal{K}$.

IV. Stiffness modulation

The springs and dampers in the I-LIP are used to apply forces on the COM of the robot during the footstep planning phase. This leads to the correction of the footstep pattern based on these forces. We hypothesize that using constant parameters for these springs and dampers will not lead to the desired compliant behavior between the object and the robot, due to the discrepancy between the forces the COM actually experiences and the forces predicted by the springs and dampers.

The stiffness of the x-component spring is updated in every loop of the low-level control as:

$$K^{\mathrm{x}}_t = K^{\mathrm{x}}_t - k^{\mathrm{x}}_1(x^{\mathrm{b}}(t) - x^{\mathrm{c}}(t) - x^{\mathrm{b}}_{\mathrm{A}}(t) + x^{\mathrm{c}}_{\mathrm{A}}(t)) - b^{\mathrm{x}}_1(\dot{x}^{\mathrm{b}}(t) - \dot{x}^{\mathrm{c}}(t) - \dot{x}^{\mathrm{b}}_{\mathrm{A}}(t) + \dot{x}^{\mathrm{c}}_{\mathrm{A}}(t)) \quad (24)$$

Here, $x^{\mathrm{c}}_{\mathrm{A}}(t)$ and $\dot{x}^{\mathrm{c}}_{\mathrm{A}}(t)$ are the desired x components of position and velocity of the robot's COM for achieving the desired compliant behavior given by the admittance model. Similarly, $x^{\mathrm{b}}_{\mathrm{A}}(t)$ and $\dot{x}^{\mathrm{b}}_{\mathrm{A}}(t)$ are the desired x components of position and velocity of the object's COM for achieving the desired compliant behavior given by the admittance model. These desired values are computed using the function f_{a} from (6) as:

$$x^{\mathrm{c}}_{\mathrm{A}}(t), \dot{x}^{\mathrm{c}}_{\mathrm{A}}(t) = f_{\mathrm{a}}(x^{\mathrm{c}}_{\mathrm{A}}(t-\delta t), \dot{x}^{\mathrm{c}}_{\mathrm{A}}(t-\delta t), x^{\mathrm{b}}_{\mathrm{A}}(t-\delta t), v^{\mathrm{bx}}_{\mathrm{d}}, \delta t) \quad (25)$$

$$x^{\mathrm{b}}_{\mathrm{A}}(t) = x^{\mathrm{b}}_{\mathrm{A}}(t) + v^{\mathrm{bx}}_{\mathrm{d}}\delta t \quad (26)$$

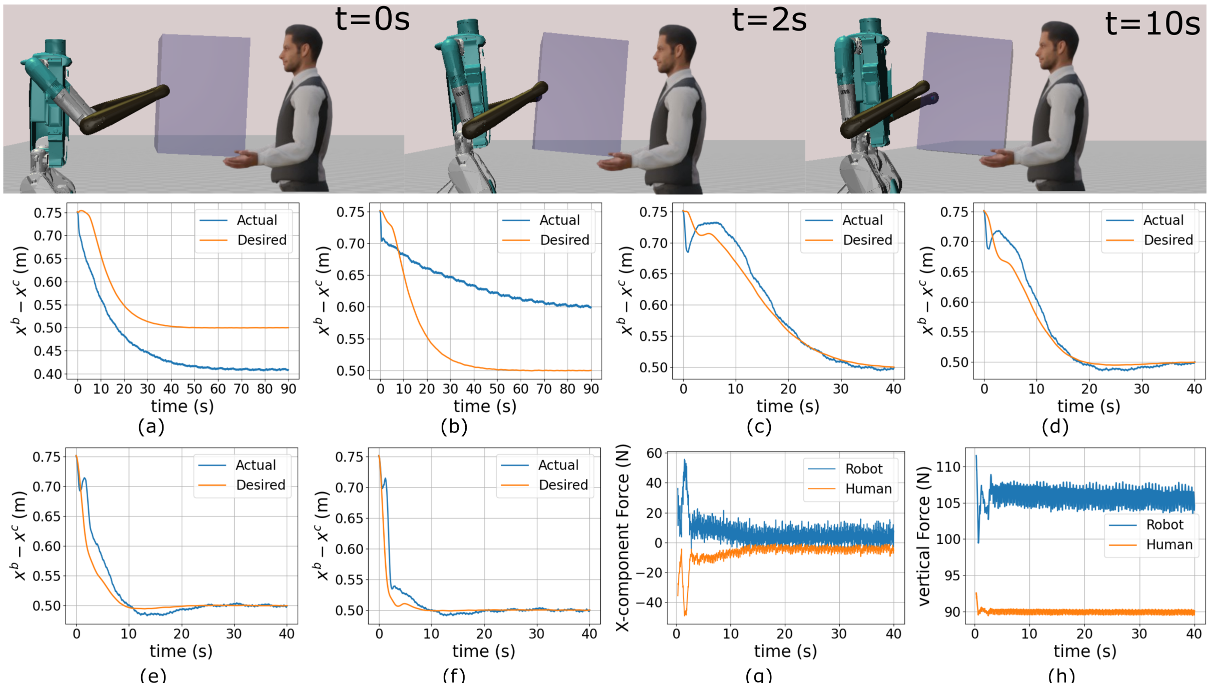

Fig. 3: (a,b) Distance between the COM of robot and object without stiffness modulation and constant I-LIP spring stiffness of 10N/m and 40N/m, respectively. (c,d,e,f) Distance between the COM of robot and object with stiffness modulation of the I-LIP spring. The stiffness is equal to $K_{\mathrm{a}}^{\mathrm{x}} = 10$ N/m, $K_{\mathrm{a}}^{\mathrm{x}} = 20$ N/m, $K_{\mathrm{a}}^{\mathrm{x}} = 60$ N/m, and $K_{\mathrm{a}}^{\mathrm{x}} = 120$ N/m respectively. (g) Low-pass filtered x- component interaction forces of robot and human with the box for $K_{\mathrm{a}}^{\mathrm{x}} = 120$ N/m (h) Low-pass filtered vertical load experienced by the robot and the human.

Here, δt is the time duration between two consecutive instances of low level control. At $t = 0$, we set $x_{\mathrm{A}}^{\mathrm{c}}(0)$ equal to $x^{\mathrm{c}}(0)$, $\dot{x}_{\mathrm{A}}^{\mathrm{c}}(0)$ equal to $\dot{x}^{\mathrm{c}}(0)$ and $x_{\mathrm{A}}^{\mathrm{b}}(0)$ equal to $x_{\mathrm{b}}(0)$. The updated stiffness is fed to the high-level and low-level control at required frequencies, as shown in Fig. 1.

V. Results

We validate the proposed framework in collaborative transport task in simulation (MuJoCo). The collaboration task consists of the human as a leader, Digit as a follower, and both collaborating to carry an object in a straight line. The leader intends to move the box at a constant speed in a straight line, and it is modeled using a PD controller with high damping. The robot has no knowledge of this speed. The leader also intends to maintain the object orientation equal to identity quaternion. The follower's (Digit) goal is to exhibit desired compliant behavior with respect to the box while maintaining stable locomotion. The robot takes on 55% (approx. 11 kg) of the vertical load while the human takes on the rest (9 kg).

The results of the application of our control framework in this collaboration are shown in Fig. 3. In this simulation, the human intends to move the box with a speed of 0.2 m/s, and the spring in the admittance model has a stiffness of 10 N/m and a natural length of 0.5 m. Figure 3(a) and (b) show the distance between the COM of robot and object without stiffness modulation and constant I-LIP spring stiffness of 10 N/m and 40 N/m, respectively. As shown, the lack of stiffness modulation leads to tracking error in the distance between the robot and the box. However, when the proposed stiffness modulation is used, the tracking error is minimized, as shown in Fig. 3(c)-(f). Specifically, Fig. 3(c)-(f) show the tracking performance when the admittance model stiffness is set equal to $K_{\mathrm{a}}^{\mathrm{x}} = 10\ N/m$, $K_{\mathrm{a}}^{\mathrm{x}} = 20\ N/m$, $K_{\mathrm{a}}^{\mathrm{x}} = 60\ N/m$, and $K_{\mathrm{a}}^{\mathrm{x}} = 120\ N/m$ respectively. Moreover, the distances all converge to the natural length of the springs, which leads to the minimization of interaction forces between the robot and the human. This is also shown in Fig. 3(g), where the interaction forces between the human and the object are less than 10 N except for the initial phase, while the forces between the robot and the box are also relatively low. Finally, Fig. 3(h) shows the vertical load distribution between the robot and the human, which is what was intended by design.

VI. Conclusions

We have presented an MPC-QP type control framework with stiffness modulation for physical human-humanoid collaboration that is validated through a collaborative object transfer. The framework includes an admittance controller above the MPC, while it introduces the I-LIP model for motion planning in the MPC. The generated footstep plan enables the robot to exhibit compliant behavior around the object, while the low-level QP realizes this plan on the robot. The QP is informed of the object dynamics, and therefore it has the ability to control the interaction forces between the object and the robot. With stiffness modulation, the performance of the framework is validated in simulation, in terms of tracking performance for different levels of compliance between the robot and the object, while minimizing interaction forces with the human. The proposed framework surpasses the current state of the art in human-humanoid collaboration controllers, enabling effective interaction in applications including collaborative transport, among others.

References

[1] N. Jarrassé, T. Charalambous, and E. Burdet, "A framework to describe, analyze and generate interactive motor behaviors," *PLOS ONE*, vol. 7, no. 11, pp. 1–13, 11 2012.

[2] M. Huber, M. Rickert, A. Knoll, T. Brandt, and S. Glasauer, "Human-robot interaction in handing-over tasks," in *RO-MAN 2008 - The 17th IEEE International Symposium on Robot and Human Interactive Communication*, 2008, pp. 107–112.

[3] A. Edsinger and C. C. Kemp, "Human-robot interaction for cooperative manipulation: Handing objects to one another," in *RO-MAN 2007 - The 16th IEEE International Symposium on Robot and Human Interactive Communication*, 2007, pp. 1167–1172.

[4] J. DelPreto and D. Rus, "Sharing the load: Human-robot team lifting using muscle activity," in *2019 International Conference on Robotics and Automation (ICRA)*, 2019, pp. 7906–7912.

[5] L. Rozo, S. Calinon, and D. G. Caldwell, "Learning force and position constraints in human-robot cooperative transportation," in *The 23rd IEEE International Symposium on Robot and Human Interactive Communication*, 2014, pp. 619–624.

[6] M. Mujica, M. Crespo, M. Benoussaad, S. Junco, and J.-Y. Fourquet, "Robust variable admittance control for human–robot co-manipulation of objects with unknown load," *Robotics and Computer-Integrated Manufacturing*, vol. 79, p. 102408, 2023.

[7] K. Kosuge, M. Sato, and N. Kazamura, "Mobile robot helper," in *Proceedings 2000 ICRA. Millennium Conference. IEEE International Conference on Robotics and Automation. Symposia Proceedings (Cat. No.00CH37065)*, vol. 1, 2000, pp. 583–588 vol.1.

[8] K. Kosuge, H. Kakuya, and Y. Hirata, "Control algorithm of dual arms mobile robot for cooperative works with human," in *2001 IEEE International Conference on Systems, Man and Cybernetics. e-Systems and e-Man for Cybernetics in Cyberspace (Cat.No.01CH37236)*, vol. 5, 2001, pp. 3223–3228 vol.5.

[9] R. Suda and K. Kosuge, "Handling of object by mobile robot helper in cooperation with a human using visual information and force information," in *IEEE/RSJ International Conference on Intelligent Robots and Systems*, vol. 2, 2002, pp. 1102–1107 vol.2.

[10] H. Xing, A. Torabi, L. Ding, H. Gao, W. Li, V. K. Mushahwar, and M. Tavakoli, "Human-robot collaboration for heavy object manipulation: Kinesthetic teaching of the role of wheeled mobile manipulator," in *2021 IEEE/RSJ International Conference on Intelligent Robots and Systems (IROS)*, 2021, pp. 2962–2969.

[11] W. Li, P. Li, L. Jin, R. Xu, J. Guo, and J. Wang, "Compliant-control-based assisted walking with mobile manipulator," *Biomimetics*, vol. 9, no. 2, p. 104, 2024.

[12] K. Yokoyama, H. Handa, T. Isozumi, Y. Fukase, K. Kaneko, F. Kanehiro, Y. Kawai, F. Tomita, and H. Hirukawa, "Cooperative works by a human and a humanoid robot," in *2003 IEEE International Conference on Robotics and Automation (Cat. No.03CH37422)*, vol. 3, 2003, pp. 2985–2991 vol.3.

[13] D. J. Agravante, A. Cherubini, A. Bussy, P. Gergondet, and A. Kheddar, "Collaborative human-humanoid carrying using vision and haptic sensing," *2014 IEEE International Conference on Robotics and Automation (ICRA)*, pp. 607–612, 2014.

[14] K. S. Narkhede, A. M. Kulkarni, D. A. Thanki, and I. Poulakakis, "A sequential MPC approach to reactive planning for bipedal robots using safe corridors in highly cluttered environments," *IEEE Robotics and Automation Letters*, vol. 7, no. 4, pp. 11 831–11 838, 2022.

[15] S. Kajita, F. Kanehiro, K. Kaneko, K. Yokoi, and H. Hirukawa, "The 3D linear inverted pendulum mode: a simple modeling for a biped walking pattern generation," in *Proceedings 2001 IEEE/RSJ International Conference on Intelligent Robots and Systems. Expanding the Societal Role of Robotics in the the Next Millennium (Cat. No.01CH37180)*, vol. 1, 2001, pp. 239–246 vol.1.

[16] Y. Ding, C. Khazoom, M. Chignoli, and S. Kim, "Orientation-aware model predictive control with footstep adaptation for dynamic humanoid walking," in *2022 IEEE-RAS 21st International Conference on Humanoid Robots (Humanoids)*, 2022, pp. 299–305.

[17] Q. Nguyen and K. Sreenath, "Safety-critical control for dynamical bipedal walking with precise footstep placement," *IFAC-PapersOnLine*, vol. 48, no. 27, pp. 147–154, 2015.

[18] D. J. Agravante, A. Sherikov, P.-B. Wieber, A. Cherubini, and A. Kheddar, "Walking pattern generators designed for physical collaboration," in *2016 IEEE International Conference on Robotics and Automation (ICRA)*, 2016, pp. 1573–1578.

[19] D. J. Agravante, A. Cherubini, A. Sherikov, P.-B. Wieber, and A. Kheddar, "Human-humanoid collaborative carrying," *IEEE Transactions on Robotics*, vol. 35, no. 4, pp. 833–846, 2019.

[20] P. J. Brockwell and R. A. Davis, *Introduction to time series and forecasting*. Springer, 2002.

[21] T. Koolen, T. de Boer, J. Rebula, A. Goswami, and J. Pratt, "Capturability-based analysis and control of legged locomotion, part 1: Theory and application to three simple gait models," *The International Journal of Robotics Research*, vol. 31, no. 9, pp. 1094–1113, 2012.

[22] J. Reher and A. D. Ames, "Inverse dynamics control of compliant hybrid zero dynamic walking," in *2021 IEEE International Conference on Robotics and Automation (ICRA)*, 2021, pp. 2040–2047.

[23] S. Caron, Q. C. Pham, and Y. Nakamura, "Stability of surface contacts for humanoid robots: Closed-form formulae of the contact wrench cone for rectangular support areas," *Proceedings - IEEE International Conference on Robotics and Automation*, vol. 2015, 01 2015.